Available online at www.sciencedirect.com
ScienceDirect
Journal of Power Sources 172 (2007) 404–409
JOURNAL OF POWER SOURCES
www.elsevier.com/locate/jpowsour

Short communication

Surface layer formed on silicon thin-film electrode in lithium bis(oxalato) borate-based electrolyte

Nam-Soon Choi *, Kyoung Han Yew, Ho Kim, Sung-Soo Kim, Wan-Uk Choi

Corporate R&D Center, Samsung SDI Co. Ltd., 428-5, Gonse-dong, Giheung-gu, Yongin-si, Gyeonggi-do 446-577, Republic of Korea

Received 30 April 2007; received in revised form 22 June 2007; accepted 18 July 2007
Available online 3 August 2007

Abstract

A Si thin-film electrode of 200 nm is prepared using E-beam evaporation and deposition on copper foil. The use of a lithium bis(oxalato) borate (LiBOB)-based electrolyte markedly improves the discharge capacity retention of a Si thin-film electrode/Li half-cell during cycling. The surface layer formed on Si thin-film electrode in ethylene carbonate/diethyl carbonate (3/7) with 1.3 M $LiPF_6$ or 0.7 M LiBOB is characterized by means of Fourier transform infrared spectroscopy and X-ray photoelectron spectroscopic analysis. The surface morphology of the electrode after cycling is investigated using scanning electron microscopy. The relationship between the physical morphology and the electrochemical performance of Si thin-film electrode is discussed.

Keywords: Silicon thin-film electrode; Lithium bis(oxalato) borate; Surface chemistry; Surface morphology; Lithium-ion battery capacity retention

1. Introduction

Silicon-based materials with high theoretical specific capacity (approximately 4200 mAh g^{-1} for $Li_{22}Si_5$) have been studied extensively as novel anode materials for use in lithium-ion batteries, i.e., as a substitute for graphite which has the theoretical capacity of 372 mAh g^{-1} [1,2]. These materials cannot, however, retain high capacity both because of the loss of electrical conduction paths caused by a large volume change, and because of the continuous formation of a solid electrolyte interface (SEI) film due to crack formation during repeated cycling [3–5].

The characteristics of the surface layer formed on the Si-based anode represent a key parameter that influences the kinetics of lithiation–delithiation and the interfacial stability during long-term cycling. Because the formation of the surface layer is attributed to the electrochemical reduction of the organic solvents and salts, its morphology and composition depend strongly on the electrolyte components [6–10].

The electrolyte that is commonly used in commercial Li-ion batteries is lithium hexafluorophosphate ($LiPF_6$) in a mixture of organic solvents.

In solvents, the PF_6^- anion undergoes an equilibrium, i.e.,

$$LiPF_6(sol.) \leftrightarrow LiF(s) + PF_5(sol.), \quad (1)$$

where the strong Lewis acid PF_5 tends to react with organic solvents, and labile P–F bonds are highly susceptible to hydrolysis even if trace amounts of moisture are present in the electrolyte solution [11,12], i.e.,

$$LiPF_6(sol.) + H_2O \rightarrow POF_3(sol.) + LiF(s) + 2HF(sol.) \quad (2)$$

$$PF_5(sol.) + H_2O \rightarrow POF_3(sol.) + 2HF(sol.) \quad (3)$$

The resulting HF reacts with the Si phase (reaction (4)), and thereby leads to the formation of cracks in the Si–Si network.

$$Si + 4HF + 2F^- + 2h^+ \rightarrow SiF_6^{2-} + 2H^+ + H_2(g) \quad (4)$$

This means that Si-based active materials become electrochemically inactive and thereby the capacity utilization in $LiPF_6$-based electrolyte decreases.

Much effort has been devoted to the formation of an electrochemically stable surface layer between the anode and the electrolyte solution. Recently, the application of lithium bis(oxalato) borate (LiBOB) has been patented by Lischka et al. [13] and developed by Xu and Angell [14] as a potential replacement for $LiPF_6$. Many unique uses of LiBOB have been reported,

* Corresponding author. Fax: +82 31 210 7555.
E-mail address: ns75.choi@samsung.com (N.-S. Choi).

0378-7753/$ – see front matter © 2007 Elsevier B.V. All rights reserved.
doi:10.1016/j.jpowsour.2007.07.058

namely: stabilization of the surface layer formed on the surface of a graphite anode [15]; prevention of PC co-intercalation by forming a protective film on graphite [16,17]; improvement of the high-temperature performance of Li-ion batteries [11,12].

In this study, an attempt is made to stabilize the interface between a Si thin-film electrode and the electrolyte solution through the use of LiBOB salts. Fourier transform infrared (FT-IR) and X-ray photoelectron spectroscopy (XPS) are employed to understand the effect of LiBOB-based electrolytes on the surface chemistry of the Si thin-film anode. In addition, the morphology of the surface layer formed on the Si thin-film anode is examined by means of scanning electron microscopy (SEM).

2. Experimental

A Si thin-film electrode of 200-nm thickness was prepared by means of E-beam evaporation. Deposition of the Si film was performed in a stainless-steel vessel at a working pressure of approximately 1×10^{-6} Torr. Part of the target surface was heated to its melting point using an E-beam evaporation system, which includes a cooled sample holder and an E-beam gun. The distance between the surface of the substrate and the target was 10 cm. The Si thin film was deposited on the surface of a copper foil (5 cm × 5 cm × 0.0011 cm) at room temperature using a silicon (99.99%) target. The substrate was cleaned chemically.

Electrolyte solutions of 1.3 M lithium hexafluoro phosphate ($LiPF_6$) and 0.7 M lithium bis(oxalato) borate (LiBOB) dissolved in ethylene carbonate (EC) and diethyl carbonate (DEC) (3/7, v/v) were provided by Cheil Industry.

The surface morphology of the Si thin-film electrode in LiBOB-based or $LiPF_6$-based electrolyte solution was investigated by means of SEM (JEOL JSM-6700F). The surface layers were characterized with XPS (ESCA LAB 250), in which an Al Kα excitation source was used, and *ex situ* FT-IR (BRUKER EQUINOX 55) at a spectral resolution of 4 cm^{-1}. The procedures were as follows. After cycling, cells were carefully opened in a glove box. The electrodes were recovered, rinsed in dimethyl carbonate (DMC) to remove residual electrolyte solution, and then dried under vacuum at room temperature for 5 h. A vacuum sample transporter with an airtight adaptor was used to load the dried samples into the XPS target chamber, and FT-IR analysis was performed in a dry room (dew point <−60 °C).

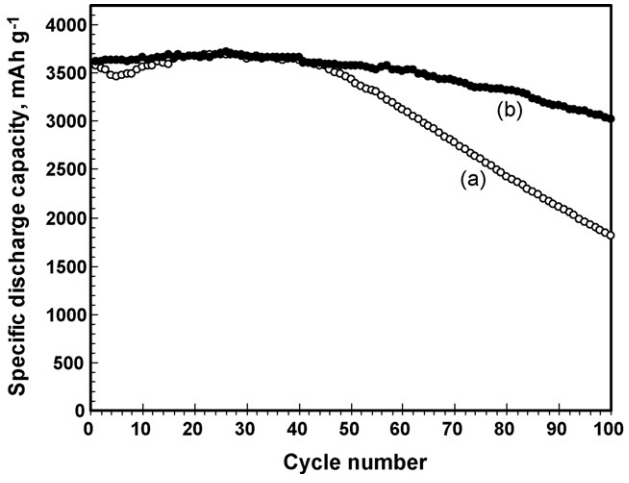

Fig. 1. Discharge capacity retention of Si|Li half-cell containing: (a) EC/DEC (3/7) 1.3 M $LiPF_6$; (b) EC/DEC (3/7) 0.7 M LiBOB during 100 cycles. Charge cut-off: 0.005 V CC mode, discharge cut-off: 2.0 V CC mode; current rate during cycling: C/5.

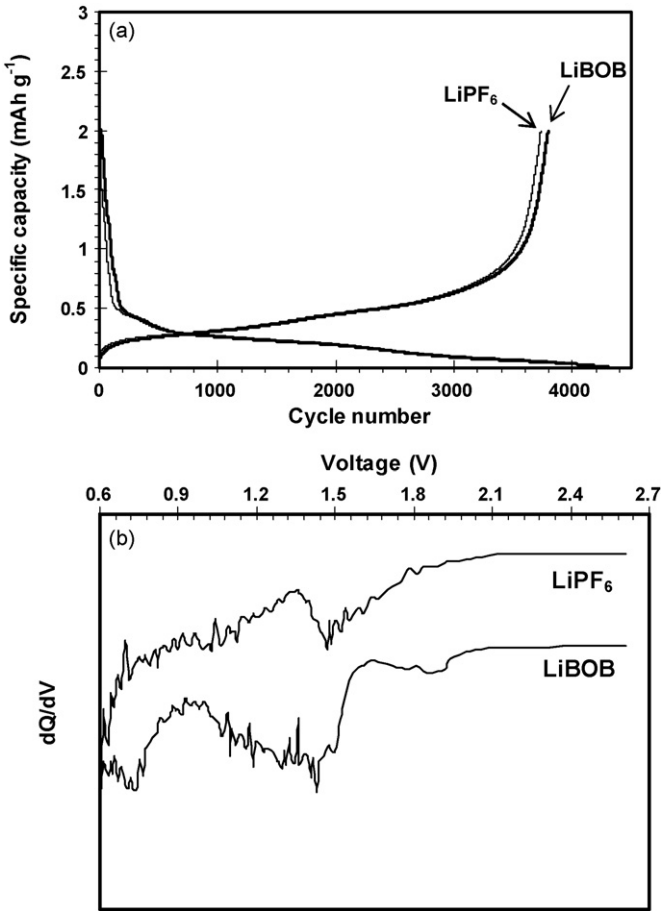

Fig. 2. (a) Charge and discharge curves at pre-cycling. (b) dQ/dV plots of Si|electrolyte|Li half-cell containing EC/DEC (3/7) 1.3 M $LiPF_6$ and EC/DEC (3/7) 0.7 M LiBOB at pre-cycling. Charge cut-off: 0.005 V CC mode; discharge cut-off: 2.0 V CC mode; current rate during cycling: C/10.

The electrochemical properties of the Si thin-film electrode were examined using a pouch half-cell (electrode area: 1 cm × 1 cm). The half-cells were fabricated by sandwiching a polyethylene separator (30 μm) between the Si thin-film electrode and metallic lithium (100 μm, Cyprus Foote Mineral Co., USA). The separator contained the electrolyte solution. Charge–discharge tests of the Si|Li half-cells were conducted

Table 1
Initial coulombic efficiency and capacity retention after 100 cycles of after Si|electrolyte|Li half-cell with different electrolyte solutions

	EC/DEC (3/7) 1.3 M $LiPF_6$	EC/DEC (3/7) 0.7 M LiBOB
Initial coulombic efficiency (%)	87.8	88.1
Discharge capacity retention (%)	50.8	83.5

over the voltage range of 0.005–2.0 V using a galvanostat (TOSCAT-3000, Toyo system, Co.) to provide a constant current density (CC) of 0.04 mA cm^{-2} (C/5 rate). A Si thin-film electrode of 200 nm gave a capacity of 0.22 mAh cm^{-2} based on the theoretical specific capacity of 4000 mAh g^{-1} for $Li_{4.2}Si$.

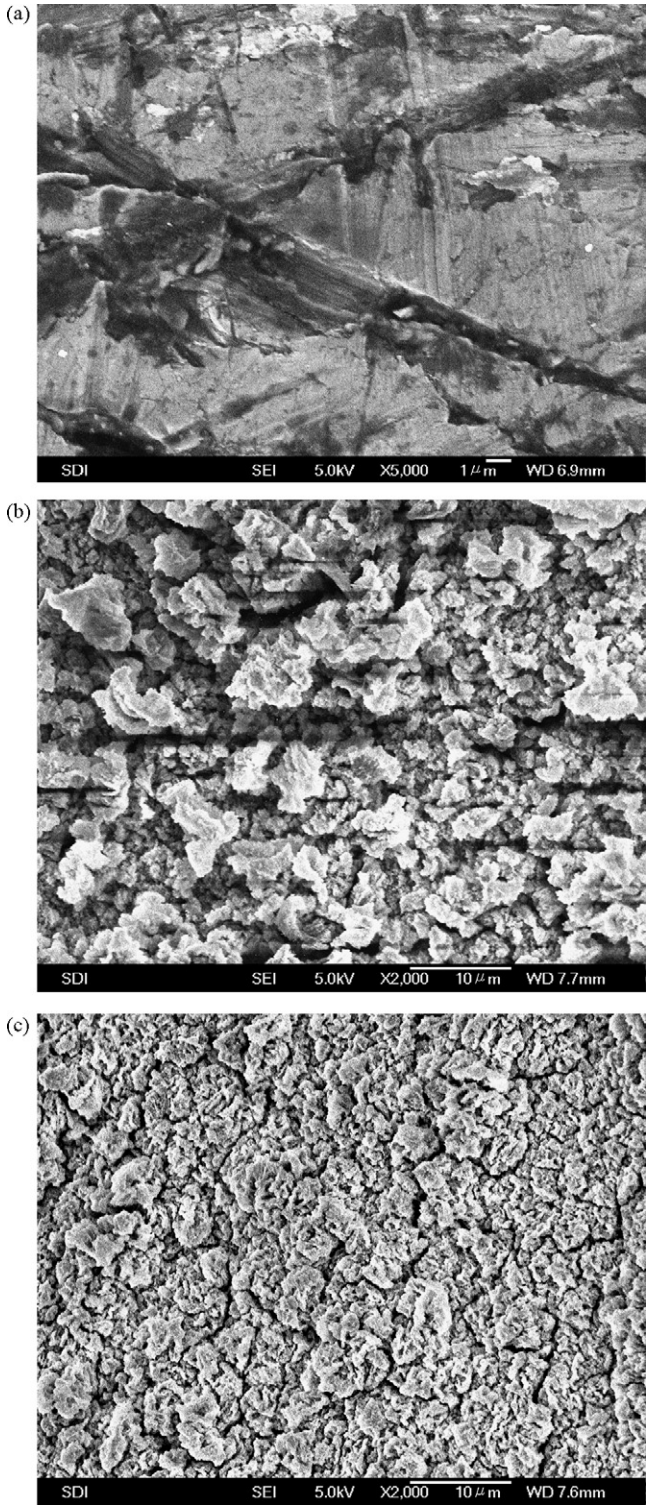

Fig. 3. Scanning electron micrographs of surface morphology of silicon thin-film electrode: (a) before cycling; after 80 cycles in (b) EC/DEC (3/7) 1.3 M $LiPF_6$; (c) EC/DEC (3/7) 0.7 M LiBOB.

3. Results and discussion

3.1. Electrochemical performance of Si/Li half-cell in $LiPF_6$ and LiBOB-based electrolyte solutions

The discharge capacity of a Si|Li half-cell containing EC/DEC (3/7) with 1.3 M $LiPF_6$ decays dramatically after 40 cycles, as shown in Fig. 1. This means that the irreversible reaction in which active lithium ions are consumed occurs continuously with cycling. On the other hand, the discharge capacity retention of the Si|Li half-cell is improved by using EC/DEC (3/7) with 0.7 M LiBOB.

The initial coulombic efficiency (ICE) of the half-cell containing EC/DEC (3/7) with 0.7 M LiBOB is higher than that of the cell with the $LiPF_6$-based electrolyte, as illustrated in Fig. 2(a) and Table 1. This indicates that a LiBOB-based electrolyte can reduce lithium consumption by trapping the lithium in the Si thin-film electrode and forming a surface layer. The irreversible capacity and the cycling behaviour are closely linked to the characteristics of the surface layer. Reductive decomposition of LiBOB clearly progresses before that of EC and $LiPF_6$. It is proposed that the LiBOB-originated surface layer, which is formed at the Si|electrolyte interface, effectively diminishes the chemical or electrochemical reaction between HF and the Si phase and thereby limits the formation of cracks. Consequently, it is concluded that the LiBOB-based electrolyte has improved the cycling properties of the Si|Li half-cell.

3.2. Characterization of $LiPF_6$- and LiBOB-originated surface layers

In order to explain the difference in cycling behaviour in different electrolytes, the surface morphologies of silicon thin-film electrodes cycled in $LiPF_6$- and LiBOB-based electrolytes were investigated.

A Si thin-film electrode cycled in the $LiPF_6$-based electrolyte has a moss-like, porous structure after 80 cycles, as shown in Fig. 3(b). This may result from cracking of the active Si phase

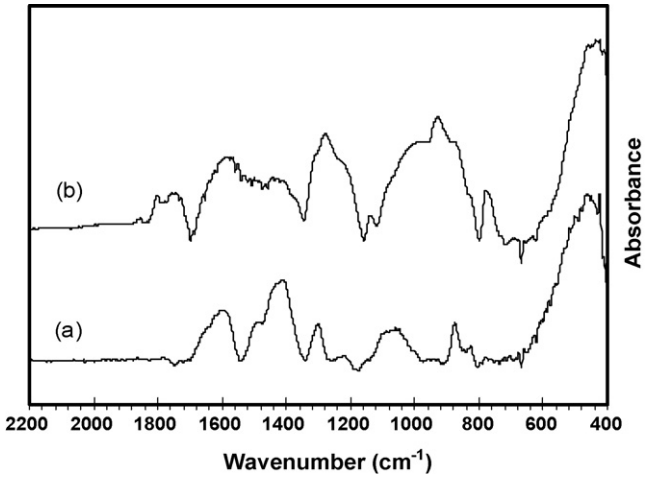

Fig. 4. FT-IR spectra for silicon thin-film electrode cycled in (a) EC/DEC (3/7, v/v) 1.3 M $LiPF_6$ and (b) EC/DEC (3/7, v/v) 0.7 M LiBOB (after 100 cycles).

caused by reaction of HF with Si–Si active sites. Cracking of a new surface layer may cause an increase in the side-reaction with the electrolyte. As a result, a continuous SEI-filming process resulting from the exposure of the new surface layer to the electrolyte results in the rapid decay in the capacity of a Si thin-film electrode in $LiPF_6$-based electrolyte [5,18]. A less-porous structure is observed for a Si thin-film electrode after 80 cycles in EC/DEC (3/7) with 0.7 M LiBOB (see Fig. 3(c)). The surface layer effectively reduces cracking of the Si active phase electrode under repeated cycling, as shown in Fig. 3(c). In summary, the

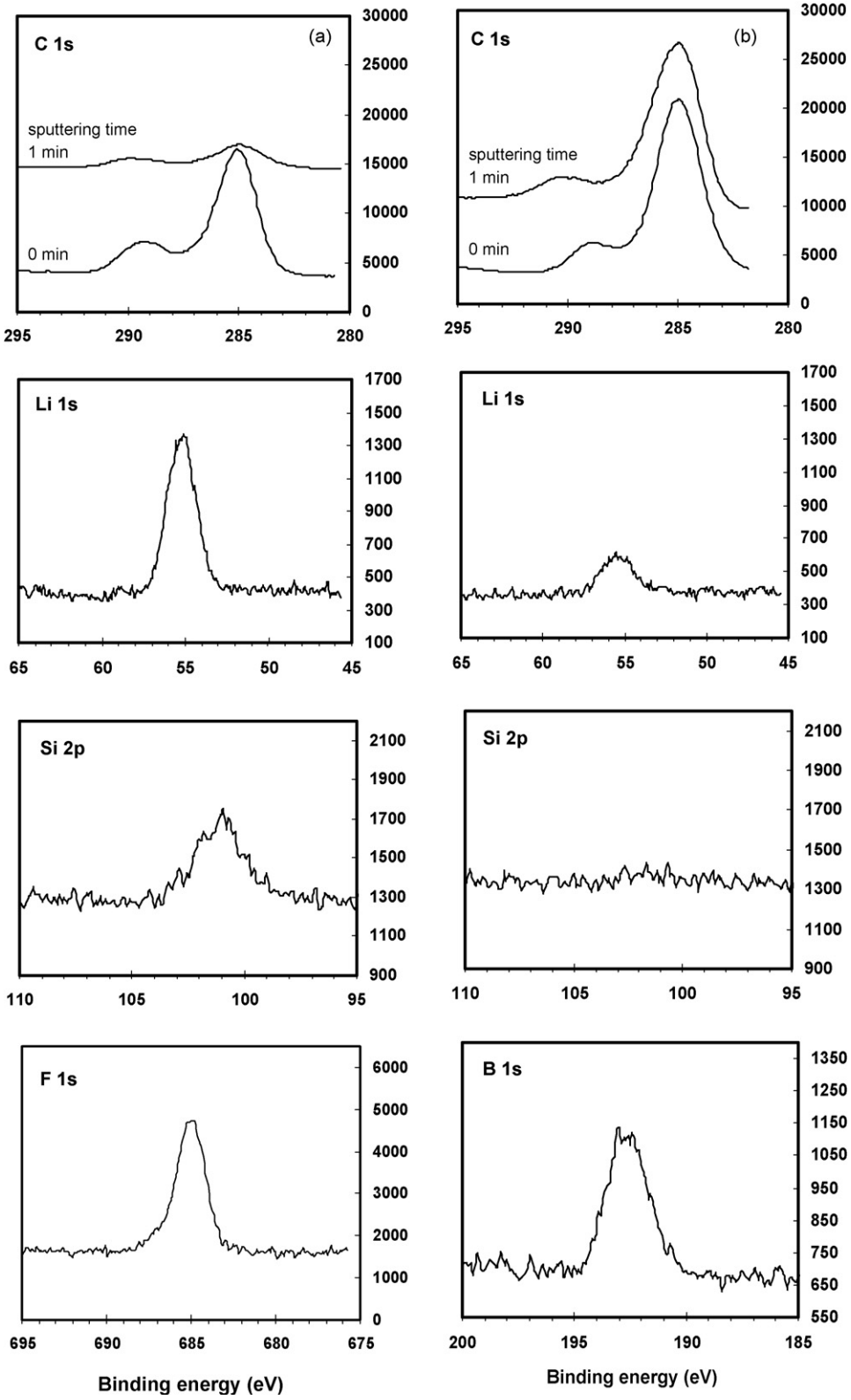

Fig. 5. XPS spectra for surface of silicon thin-film electrode cycled in (a) EC/DEC (3/7, v/v) 1.3 M $LiPF_6$ and (b) EC/DEC (3/7, v/v) 0.7 M LiBOB (after 100 cycles).

cycling properties of Si thin-film electrodes depend strongly on the physical structure of the surface layer formed by electrolyte decomposition.

Fig. 4 presents the FT-IR spectra of the surface layers formed on Si thin-film electrodes cycled in EC/DEC with 1.3 M $LiPF_6$ or 0.7 M LiBOB. For the EC/DEC/$LiPF_6$ electrolyte solution, absorption peaks corresponding to Li_2CO_3 (1508, 1431, and 868 cm^{-1}) and $ROCO_2Li$ (1650, 1400, 1300, and 1070 cm^{-1}) are observed, as shown in Fig. 4(a). It has been reported [9] that lithium alkylcarbonates ($ROCO_2Li$, called semicarbonate) are formed on the anode surface by a single-electron reaction for the electrochemical reduction of ethylene carbonate (EC). The formation of Li_2CO_3 is considered to occur via two pathways. First, electrochemical reduction EC with lithium ion

$$EC + 2e^- + 2Li^+ \rightarrow Li_2CO_3 + CH_2{=}CH_2 \quad (5)$$

and second, chemical reaction of $ROCO_2Li$ with trace water [19,20]

$$2ROCO_2Li + H_2O \rightarrow Li_2CO_3 + 2ROH + CO_2 \quad (6)$$

In the present study, the surface layer formed on the Si thin-film electrode in EC/DEC with 0.7 M LiBOB reveals a unique surface chemistry in that it has never been observed in case of EC/DEC with 1.3 M LiF_6. From the results of FT-IR analysis, it is found that the absorption peaks appearing at 1640, 1320 and 780 cm^{-1} originate from lithium oxalate formed by the reductive decomposition of BOB^- anions [15,21]. A three-coordinated borate produced by the ring-opening process of the BOB^- anion is observed at 1280 cm^{-1}, which corresponds to the O–B–O bending modes, the peak at 989 cm^{-1} is associated with the O–B–O asymmetric stretching modes. When the LiBOB-based electrolyte is used, the formation of a three-coordinated borate (192–193 eV) at the interface between the Si thin-film electrode and the electrolyte is again confirmed by XPS analysis, as shown in Fig. 5(b). The pronounced peaks at 1800 and 1760 cm^{-1} are indicative of C=O stretching in unreacted BOB anions, as shown in Fig. 4(b) [15].

Fig. 5 shows the XPS spectra of the surface layer formed on a Si thin-film electrodes cycled in EC/DEC with 1.3 M $LiPF_6$ or in EC/DEC with 0.7 M LiBOB. A peak at 289 eV assigned to semicarbonate is observed for both electrolytes. After Ar^+ sputtering for 1 min of the surface layer formed in EC/DEC/$LiPF_6$, the peak of the semicarbonate almost disappears compared with the surface layer formed in LiBOB-based electrolyte. From the results of XPS analysis, it is concluded that the semicarbonate produced by the reductive decomposition of BOB^- anions is abundant in the LiBOB-originated surface layer.

With respect to the Li 1s spectrum, the signals corresponding to Li_2CO_3, LiOH and Li_2O in LiBOB-based electrolyte show lower intensity than those for a $LiPF_6$-based electrolyte. This means that the LiBOB-originated surface layer consists mainly of the reduction products of the BOB^- anions and that it is formed by the reductive decomposition of EC molecules in $LiPF_6$-based electrolyte.

With the EC/DEC (3/7) with 0.3 M $LiPF_6$ electrolytes, the signals corresponding to silicon (Si^0: 99.8 eV) and silicon oxide

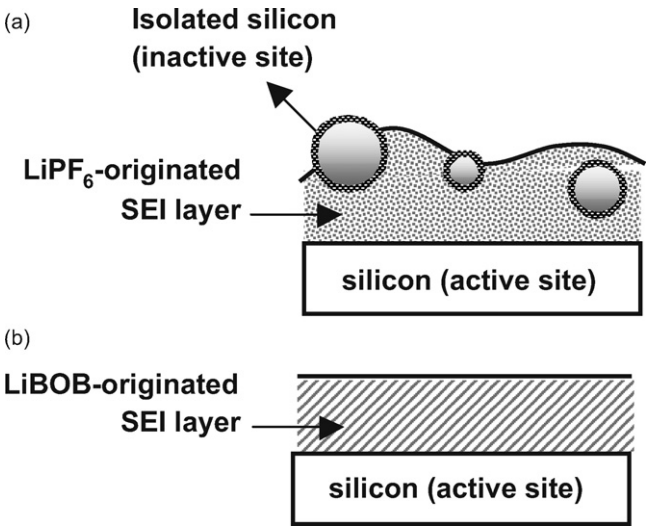

Fig. 6. Schematic illustration of surface layer formed on silicon phase cycled in (a) EC/DEC (3/7, v/v) 1.3 M $LiPF_6$ and (b) EC/DEC (3/7, v/v) 0.7 M LiBOB.

(Si^+: 101, Si^{2+}: 102, Si^{3+}: 103, and Si^{4+}: 104 eV) obviously appear at the surface layer, as shown in Fig. 5(a) [22]. This indicates that the surface layer contains the Si-based components, and becomes electrochemically inactive by the loss of electronic conducting paths during cycling, as shown schematically in Fig. 6(a). It is suggested that the cracks in the Si thin-film electrode are due to the formation of a Si–F phase through the chemical or electrochemical reaction of HF in the $LiPF_6$-based electrolyte with the Si active phase. The cracks propagate continuously during cycling, with consequent crumbling of the Si thin-film. The separated Si particles become covered with a SEI layer on prolonged cycling. The Si phase is therefore rendered inactive and causes a decay in electrode capacity.

The F 1s spectrum for the $LiPF_6$-containing electrolyte contains a core peak at 685 eV, which corresponds to LiF, and a shoulder at 687 eV, which corresponds to LiP_xF_y. Less-stable salts, such as LiP_xF_y, can consume active lithium ions by the reductive decomposition, and thereby the capacity gradually decreases on cycling [18,23].

In the case of the Si thin-film electrode cycled in EC/DEC (3/7) with 0.7 M LiBOB, the Si 2p spectra do not contain the peaks corresponding to silicon and silicon oxide. This means that an electrochemically inactive Si phase is not formed in the surface layer, as illustrated in Fig. 6(b). The LiBOB-originated surface layer is effectively maintained at the Si|electrolyte interface when there is large volume change of Si thin-film electrode during the repeated cycling, and thus the active Si phase is not exposed to the electrolyte solution.

4. Conclusions

LiBOB-based electrolyte obviously improve the discharge capacity retention of a Si|Li half-cell and also lead to the formation of a surface layer with a less-porous structure. The chemical composition of LiBOB-originated surface layer is confirmed using FT-IR and XPS analysis. The results obtained from XPS analysis show that the LiBOB-originated surface layer

effectively limits the formation of electrochemically inactive Si phases. It is found that the cyclic degradation in the capacity of the Si|Li half-cell is strongly related to the physical morphology of the surface of the Si thin-film and to the formation of inactive Si phases in the surface layer.

References

[1] J.P. Maranchi, A.F. Hepp, P.N. Kumta, Electrochem, Solid State Lett. 6 (9) (2003) A198–A201.
[2] H. Li, X. Huang, L. Chen, Z. Wu, Y. Liang, Electrochem. Solid State Lett. 2 (11) (1999) 547–549.
[3] T.D. Hatchard, J.R. Dahn, J. Electrochem. Soc. 151 (6) (2004) A838–A842.
[4] Z. Chen, V. Chevrier, L. Christensen, J.R. Dahn, Electrochem. Solid State Lett. 7 (10) (2004) A310–A314.
[5] M. Winter, J.O. Besenhard, Electrochim. Acta 45 (1999) 31–50.
[6] H. Ota, Y. Sakata, A. Inoue, S. Yamaguchi, J. Electrochem. Soc. 151 (10) (2004) A1659–A1669.
[7] H. Yoshitake, K. Abe, T. Kitakura, J.B. Gong, Y.S. Lee, H. Nakamura, M. Yoshio, Chem. Lett. 32 (2) (2003) 134–135.
[8] R. Mogi, M. Inaba, S.-K. Jeong, Y. Iriyama, T. Abe, Z. Ogumi, J. Electrochem. Soc. 149 (12) (2002) A1578–A1583.
[9] R. McMillan, H. Slegr, Z.X. Shu, W. Wang, J. Power Sources 81/82 (1999) 20–26.
[10] K.-C. Moller, H.J. Santner, W. Kern, S. Yamaguchi, J.O. Besenhard, M. Winter, J. Power Sources 119–121 (2003) 561–566.
[11] K. Xu, Chem. Rev. (Washington, DC) 104 (2004) 4303–4418.
[12] K. Xu, S.S. Zhang, T.R. Jow, W. Xu, C.A. Angell, Electrochem. Solid State Lett. 5 (1) (2002) A26–A29.
[13] U. Lischka, U. Wietelmann, M. Wegner, Ger. Pat., DE 19829030 C1 (1999).
[14] W. Xu, C.A. Angell, Electrochem. Solid State Lett. 4 (2001) E1–E4.
[15] K. Xu, U. Lee, S.S. Zhang, J.L. Allen, T.R. Jow, Electrochem. Solid State Lett. 7 (9) (2004) A273–A277.
[16] G.V. Zhuang, K. Xu, T.R. Jow, P.N. Ross, Electrochem. Solid State Lett. 7 (8) (2004) A224–A227.
[17] S.S. Zhang, K. Xu, T.R. Jow, J. Power Sources 156 (2006) 629–633.
[18] N.S. Choi, K.H. Yew, K.Y. Lee, M. Sung, H. Kim, S.S. Kim, J. Power Sources 161 (2006) 1254–1259.
[19] D. Aurbach, M.L. Daroux, P.W. Faguy, E. Yeager, J. Electrochem. Soc. 134 (1987) 1611–1620.
[20] D. Aurbach, Y. Ein-Eli, O. Chusid, Y. Carmeli, M. Babai, H. Yamin, J. Electrochem. Soc. 141 (1994) 603–611.
[21] K. Xu, U. Lee, S.S. Zhang, J.L. Allen, T.R. Jow, J. Electrochem. Soc. 151 (12) (2004) A2106–A2112.
[22] A. Hohl, T. Wieder, P.A. van Aken, T.E. Weirich, G. Denninger, M. Vidal, S. Oswald, C. Deneke, J. Mayer, H. Fuess, J. Non-Cryst. Solids 320 (1–3) (2003) 255–280.
[23] M. Herstedt, A.M. Andersson, H. Rensmo, H. Siegbahn, K. Edstrom, Electrochim. Acta 49 (2004) 4934–4947.